

Transition from inhomogeneous to homogeneous broadening at a lasing prethresholdI. S. Pashkevich ¹, I. V. Doronin,^{1,2,3} E. S. Andrianov,^{1,2,4} and A. A. Zyablovsky ^{1,2,4,5,*}¹*Moscow Institute of Physics and Technology, 9 Institutskiy pereulok, 141700 Moscow, Russia*²*Dukhov Research Institute of Automatics, 22 Sushchevskaya, 127055 Moscow, Russia*³*Institute of spectroscopy RAS, 5 Fizicheskaya, Troitsk, 108840 Moscow, Russia*⁴*Institute for Theoretical and Applied Electromagnetics, 13 Izhorskaya, 125412 Moscow, Russia*⁵*Kotelnikov Institute of Radioengineering and Electronics RAS, 11-7 Mokhovaya, 125009 Moscow, Russia*

(Received 8 December 2023; revised 28 January 2024; accepted 21 February 2024; published 6 March 2024)

The emission linewidth in active medium emerges due to homogeneous and inhomogeneous broadening. We demonstrate that in lasers with inhomogeneous broadening there is a critical pump rate, above which the special mode forms. This mode consists of locked-in oscillations of cavity mode and of the active atoms with different transition frequencies. Below the critical value of the pump rate, the radiation spectrum of the laser has a Gaussian profile, provided that inhomogeneous broadening is dominant. Above the critical value of pump rate, the special mode mostly determines the laser radiation spectrum. As a result, the spectrum attains Lorentz shape characteristic for homogeneous broadening. The formation of the special mode precedes lasing and that the critical pump rate plays the role of lasing prethreshold. We suggest a system where such a transition could be experimentally observed separately from lasing. We obtain expressions for the threshold and generation frequency of a single-mode laser where both homogeneous and inhomogeneous broadening are present.

DOI: [10.1103/PhysRevA.109.033506](https://doi.org/10.1103/PhysRevA.109.033506)**I. INTRODUCTION**

Width of emission spectrum of active medium greatly impacts behavior of any system built on this medium. Linewidth is determined by combination of two types of broadening: homogeneous and inhomogeneous. Homogeneous broadening of emission spectrum occurs due to finite lifetime of excited states of active atoms (or molecules, quantum dots, etc.) [1–5]. This contribution is dominant when all atoms of active medium are identical and therefore share transition frequency.

In contrast, inhomogeneous broadening occurs due to different transition frequencies of atoms which results in the collective spectrum being broader than the spectrum of individual atoms. This difference in frequencies can originate from various sources. It can take place because atoms have different properties, such as varying sizes of quantum dots [6–10]. In addition, the difference in size can lead to a difference in the dipole moments of the quantum dots, which causes variation of the coupling strength [11]. Other effects contributing to this type of broadening are a different environment near individual atoms like inhomogeneous electromagnetic field or lattice defects [12–15] and solute-solvent interaction [16–18]. Depending on the orientation and position of the active atoms or molecules inside such systems, they have different coupling strengths. Such a behavior can take place in random lasers [19], in plasmonic lasers [20], etc. Finally, the inhomogeneous broadening can be caused by Doppler effect originating from the difference in atoms' velocities [21–23].

The presence of inhomogeneous broadening leads to an emission spectrum with Gaussian shape [18,24,25]. This result can be explained by the central limit theorem [26], which states that the sum of independent random variables has a Gaussian distribution. In contrast, homogeneous broadening results in a Lorentzian spectrum [25,27]. However, contributions of the two types of broadening can be difficult to distinguish by the emission spectrum alone. In some cases, they are shown to behave similarly, which renders distinction redundant [28,29].

Despite superficial similarity, the two types of broadening display distinct behavior in a variety of systems. For example, it was discovered that the shape of peaks of the vacuum-field Rabi splitting in a strong coupling regime depends only on the homogeneous broadening [30]. In turn, in [31] polaritonic peaks' coherence was found to depend crucially on the type of broadening and on the shape of linewidth in general. This result can be applied to various systems, for example, semiconductor emitters coupled to optical cavities or ensembles of spins in circuit QED. In [32] materials with inhomogeneous broadening were found to offer lower optical efficiencies than homogeneous counterparts with Nd-doped active medium under diode pumping. Additionally, time-resolved transmission and reflection from an emitter displays oscillations over time in the presence of inhomogeneous broadening [33].

In this paper, we study the influence of homogeneous and inhomogeneous broadening on the lasing threshold and laser emission spectrum. On an example of a single mode laser with dominant inhomogeneous broadening we demonstrate that there is a critical pump rate of the active medium, at which a special mode forms. The special mode includes locked-in oscillations of the electromagnetic field in the cavity and of

*zyablovskiy@mail.ru

the active atoms with different transition frequencies. The rest of the eigenmodes consist of polarizations of individual active atoms slightly modified by the interaction with the cavity mode. Below the critical pump rate, all eigenmodes give comparable contributions in the laser spectrum. Therefore, the radiation spectrum has a Gaussian shape, resulting in the inhomogeneous broadening. Above the critical value, the special mode dominates in the laser spectrum and a single line with a Lorentzian profile appears in the radiation spectrum. So, the inhomogeneous broadening no longer affects the spectrum. At the same time, the lasing threshold and the generation frequency are determined by the linewidth of the inhomogeneous broadening. We show that the formation of the special mode precedes lasing and the critical pump rate plays the role of lasing prethreshold [34]. We believe our findings aid design and study of systems based on an active medium with inhomogeneous broadening.

II. MODEL OF LASER WITH INHOMOGENEOUS BROADENING

We consider a laser based on a single mode cavity and an active medium consisting of N active atoms with two working levels. The role of active atoms can be played by, for example, dye molecules [35], quantum dots [36–38], Sr atoms in the magnetic trap [39,40], etc. We designate the resonant frequency of the cavity mode as ω_a . The transition frequencies of active atoms $\omega_\sigma^{(j)}$ have a normal distribution with the expectation value ω_σ and the variance $\Delta\omega$ ($|\omega_\sigma - \omega_a| < \Delta\omega$), which is the case for many inhomogeneously broadened media [18,24,25].

We use semiclassical Maxwell-Bloch equations [41–43] for description of the laser

$$da/dt = (-\gamma_a - i\omega_a)a - i \sum_{j=1}^N \Omega_j \sigma_j, \quad (1)$$

$$d\sigma_j/dt = (-\gamma_\sigma - i\omega_\sigma^{(j)})\sigma_j + i\Omega_j a D_j, \quad (2)$$

$$dD_j/dt = (\gamma_p - \gamma_D) - (\gamma_p + \gamma_D)D_j + 2i\Omega_j(a\sigma_j^* + a^*\sigma_j). \quad (3)$$

Here a is the amplitude of electric field in the cavity; σ_j and D_j are the polarization and the population inversion of the j th active atom, the transition frequency of which is $\omega_\sigma^{(j)}$. Ω_j is the coupling strength between the cavity electric field and j th active atom. γ_a is the relaxation rate of the electric field in the cavity. γ_D is the relaxation rate of the population inversion of active atoms. γ_p is the pump rate of the active atoms. γ_σ is the dephasing rate of active atoms, which determines the width of homogeneous broadening. The index j runs from 1 to N , where N is the total number of active atoms.

Maxwell-Bloch equations (1)–(3) are derived from operator Heisenberg-Langevin equations within the mean-field approximation (or semiclassical approximation) [42]. Within this approximation, the averages from products of operators are replaced with the products of averages ($\langle \hat{a} \hat{D}_j \rangle = \langle \hat{a} \rangle \langle \hat{D}_j \rangle$, $\langle \hat{a} \hat{\sigma}_j^\dagger \rangle = \langle \hat{a} \rangle \langle \hat{\sigma}_j \rangle^*$, and $\langle \hat{a}^\dagger \hat{\sigma}_j \rangle = \langle \hat{a} \rangle^* \langle \hat{\sigma}_j \rangle$) [42]. This approach is applicable when the number of atoms is much greater than unity [42]. The inhomogeneous broadening in

these equations is described by the variation of transition frequencies of the active atoms and the variation of the coupling strengths, Ω_j [11,41].

Equations (1)–(3) can be used to model the effect of temperature on the laser operation. It is known that thermal fluctuations affect laser operation. For example, an increase in temperature can lead to a change in the band structure of semiconductors [44], which, in turn, changes the coupling strength and transition frequency in the active medium (e.g., in quantum dots). In addition, the dephasing processes in the active medium are, in particular, caused by the interaction of atoms with phonons of the medium [11,45–47], so the dephasing rate of the active atoms depends on temperature. Influence of temperature can be taken into account by considering the respective parameters as functions of temperature with specific dependencies either predicted theoretically or measured experimentally [$\Omega_j = \Omega_j(T)$, $\omega_\sigma^{(j)} = \omega_\sigma^{(j)}(T)$]. The temperature of active atoms can depend on the pumping that leads to dependence of the variations of transition frequencies and the coupling strengths on the pump rate. Such dependencies can be taken into account in Eqs. (1)–(3) by replacement $\omega_\sigma^{(j)} \rightarrow \omega_\sigma^{(j)}[T(\gamma_p)]$, etc. For the sake of simplicity, we will neglect in our calculations the dependence of temperature on the pump rate.

The thermal fluctuations in the active medium can also affect the population of the excited state [48,49]. This influence is determined by the ratio $k_B T / \hbar \omega_\sigma$ (k_B is Boltzmann's constant; \hbar is Planck's constant). In our work, we do not consider the influence of thermal fluctuations on the population of levels of the active medium, limiting ourselves to the case when $k_B T / \hbar \omega_\sigma \ll 1$.

We emphasize that Maxwell-Bloch equations are suitable for describing a broad class of systems. Depending on the values of relaxation rates and coupling strengths, Maxwell-Bloch equations can describe different types of lasers [50] from plasmonic lasers [51,52] to random lasers [19]. Similar equations can also be used to describe the operation of dressed-state lasers, in which emission originates from the transitions between the neighboring dressed states [11]. In these devices, the transition frequency is determined by the Rabi splitting.

III. FORMATION OF SPECIAL MODE

It is known that Maxwell-Bloch equations predict the existence of a threshold pump rate, above which the lasing takes place. Below the lasing threshold the stationary solution of Eqs. (1)–(3) is given as $a = \sigma_j = 0$ and $D = D_0 = (\gamma_p - \gamma_D) / (\gamma_p + \gamma_D)$ [42,43]. We perform linear stability analysis of the steady state below the lasing threshold. To this end, we use the equations for small deviations δa and $\delta \sigma_j$ from the zero stationary state ($a = \sigma_j = 0$) [34,53,54]

$$\frac{d}{dt} \begin{pmatrix} \delta a \\ \delta \sigma_j \end{pmatrix} = \begin{pmatrix} -\gamma_a - i\omega_a & -i\Omega_j \\ i\Omega_j D_0 & -\gamma_\sigma - i\omega_\sigma^{(j)} \end{pmatrix} \begin{pmatrix} \delta a \\ \delta \sigma_j \end{pmatrix}, \quad (4)$$

where the index j runs from 1 to N . We calculate the eigenvalues λ_k and the eigenmodes $\mathbf{e}_k = (a, \sigma_1, \dots, \sigma_N)^T$ of the matrix in the right side of Eq. (4) for different values of D_0 (i.e., for different pump rates) (Fig. 1).

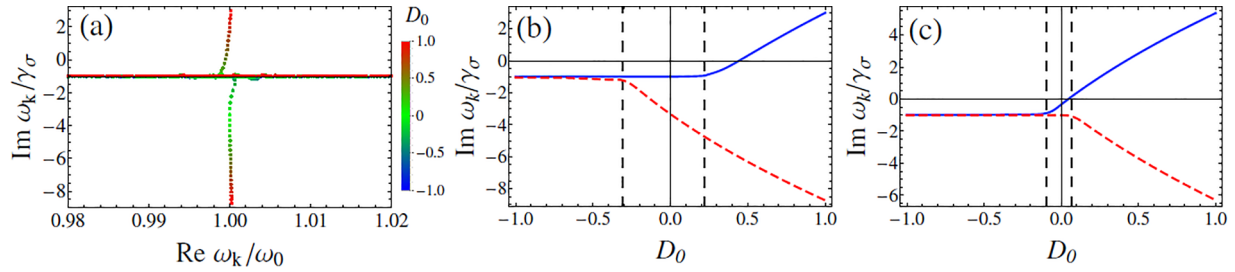


FIG. 1. (a) Trajectories of eigenfrequencies, ω_k , in the complex plane for D_0 ranging from -1 to 1 . Here $\gamma_a = 10^{-2}\omega_0$. (b), (c) Dependencies of the imaginary parts of the eigenfrequencies with the greatest (the dashed red line) and the lowest (the solid blue line) relaxation rate on D_0 when $\gamma_a = 10^{-2}\omega_0$ (b) and $\gamma_a = 10^{-3}\omega_0$ (c). $\omega_\sigma^{(j)}$ and Ω_j are independent random variables. Ω_j have a normal distribution with the expectation value $\langle\Omega\rangle$ and the variance $\Delta\Omega = 0.05\Omega$. All other parameters are the same for three figures: $N = 10^4$, $\gamma_\sigma = 3 \times 10^{-3}\omega_0$, $\langle\Omega\rangle = 3 \times 10^{-4}\omega_a$, and $\Delta\omega = 0.05\omega_\sigma$.

Hereinafter, for convenience, we consider the eigenfrequencies $\omega_k = i\lambda_k$ instead of the eigenvalues λ_k . We study the behavior of eigenfrequencies and eigenmodes with changes in the pump rate to determine the lasing threshold and changes in the spectrum of the system.

Our calculations show that in both cases when the pump rate γ_p tends to zero ($D_0 = -1$) the relaxation rates of all eigenmodes tend to γ_σ [Figs. 1(a) and 1(d)]. This is because active atoms give the main contribution to all eigenmodes. An increase in pump rate leads to a change of the relaxation rates of eigenmodes ($\text{Im } \omega_k$). Notably, there are two critical values of pump rates at which two special eigenmodes form (Fig. 1). One of these eigenmodes has the greatest relaxation rate among all eigenmodes and the other special eigenmode has the lowest relaxation rate [Figs. 1(a) and 1(d)]. When $\gamma_a > \gamma_\sigma$, the special mode with the greatest relaxation rate forms at $D_0 < 0$, whereas the other special mode forms at $D_0 > 0$ [Figs. 1(b) and 1(e)]. The opposite situation takes place when $\gamma_a < \gamma_\sigma$ [Figs. 1(c) and 1(f)].

When the pump rate exceeds both of these critical values, the special mode with the greatest relaxation rate has a negligible effect on the system dynamics because of its fast decay. Therefore, we do not consider this mode in further discussion. At the same time, the relaxation rate of the special mode with the lowest relaxation rates further decreases with the pump rate increase, as its eigenfrequency moves up in the complex plane (Fig. 1). As a result, this special mode exerts more influence on the system spectrum. It is this mode which determines behavior of the system above the critical pump rates and so we will focus on it. To clarify the mechanism of the special mode formation, we study changes in eigenmodes occurring due to the increase in pump rate. Our calculations show that, below both critical values of pump rate, each eigenmode is predominantly associated with oscillations of one of the active atoms. That is, for each eigenmode, there is a component which significantly exceeds all other components in absolute value. Above the respective critical value of pump rate, the special eigenmode with the lowest relaxation rate forms. Unlike other modes, this mode has similar absolute values of all components. Consequently, this eigenmode is associated with collective oscillations of the electromagnetic field in the cavity and of the active atoms with different transition frequencies. The formation of this special eigenmode leads to phase matching of polarizations of different

active atoms. As a result, in the special eigenmode the total polarization of all active atoms, $|\sum_j \sigma_j|$, sharply increases with the increase in pump rate above the critical pump rate [Fig. 2(a)]. Moreover, the energy flow from the active medium to the cavity, which is proportional to $\text{Im}(a^* \sum_j \sigma_j)$ [55], also increases [Fig. 2(b)]. This is accompanied by a fast decrease in relaxation rate of the special mode (Fig. 1). At the same time, for other eigenmodes the energy flow between the electric field in cavity and the active medium decreases above the critical pump rate [Fig. 2(b)]. Therefore, these eigenmodes do not experience amplification associated with the interaction between active atoms and the cavity mode; thus their relaxation rates remain close to the relaxation rate of free active atoms, γ_σ .

Thus, above the critical value of pump rate, only the relaxation rate of the special eigenmode decreases with the pump rate. When the relaxation rate of the special mode reaches zero (Fig. 1), the lasing at the special eigenmode begins. At the same time, all other eigenmodes have nonzero relaxation rates (Fig. 1). As a result, above the lasing threshold, the special mode dominates the laser spectrum. The formation of the special mode always precedes lasing. Therefore, the critical pump rate for the formation of a laser mode can be called the lasing prethreshold [34].

Note that Figs. 1 and 2 are calculated for the case when the transition frequencies and the coupling strengths are

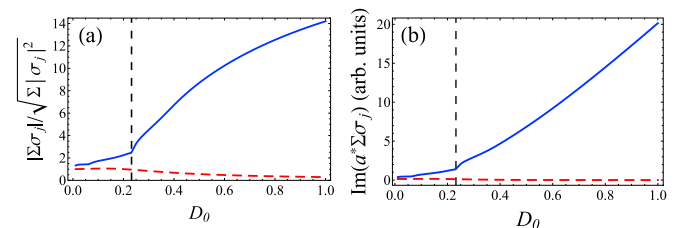


FIG. 2. (a) Dependence of the modulus of the total polarization value of all active atoms, $|\sum_j \sigma_j|$, on D_0 . The total polarization value is normalized to the square root of the sum of the squares of the polarization modules. (b) Dependence of the energy flow from the active atoms to the electromagnetic field mode. The blue lines describe the special mode; the red lines describe a typical nonspecial eigenmode. Here $\gamma_a = 10^{-2}\omega_0$. All other parameters are the same as for Fig. 1(a).

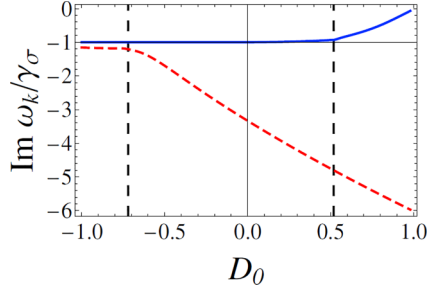


FIG. 3. Dependencies of the imaginary parts of the eigenfrequencies with the greatest (the dashed red line) and the lowest (the solid blue line) relaxation rate on D_0 . $\langle \Omega \rangle = 2 \times 10^{-4} \omega_a$. All other parameters are the same as for Fig. 1(b).

independent random variables. However, our calculations show that the obtained results persist in the presence of correlations between the random transition frequencies and the random coupling strengths (we consider the cases when $\Omega_j \sim \omega_\sigma^{(j)\alpha}$, where α ranges from -3 to 3). The presence of correlations leads to a change in the quantitative values for the critical pump rates, but ultimately does not prevent the formation of special modes.

IV. INFLUENCE OF THE SPECIAL MODE FORMATION ON THE SHAPE OF THE LASER EMISSION SPECTRUM

Formation of the special mode leads to change in the shape of the emission spectrum of the laser. Below the critical value of the pump rate all modes contribute equally to the system spectrum. Since these modes share frequencies with free active atoms (only slightly modified by the interaction with the cavity), their collective spectrum forms a Gaussian shape characteristic for inhomogeneous broadening. In contrast, above the critical value of the pump rate, the special mode dominates in the emission spectrum. Since the spectrum of a single mode has a Lorentz profile, the prevalence of the special mode in the laser spectrum leads to suppression of the inhomogeneous broadening. As a result, above the critical value of the pump rate, the laser spectrum acquires a Lorentz profile. Thus the formation of the special mode leads to the change in the shape of the spectrum.

However, the critical value of the pump rate in many systems is near the lasing threshold. Therefore, changes in the shape of the spectrum may be obscured by the transition to the lasing in experiment. To alleviate this challenge, we suggest the system where the lasing threshold is not reached. This situation can be achieved by decreasing the quality factors of the cavity or decreasing the coupling strengths between the cavity and atoms. In our calculations, we consider the cavity-atoms system, in which a Q factor of cavity is about 100 and the gain coefficient in the active medium, G , at $D_0 = 1$ is about 1800 cm^{-1} [$G = \Omega^2 N D_0 / (\gamma_\sigma c)$] [56] and $\hbar\omega_\sigma = 2 \text{ eV}$] (Fig. 3). Such parameters are typical, for example, for plasmonic lasers with the active medium based on InGaAs [57,58]. We believe that similar systems can be a good basis for observing the transition from inhomogeneous to homogeneous broadening.

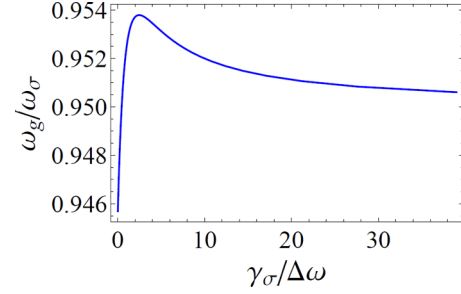


FIG. 4. Dependence of the generation frequency of the laser, ω_g , on the ratio between homogeneous width, γ_σ , and inhomogeneous width, $\Delta\omega$, when $\omega_a \neq \omega_\sigma$. The generation frequency is calculated by using Eq. (A8). Here $\gamma_a = 0.1\omega_\sigma$, $\gamma_\sigma + \Delta\omega = 0.1\omega_\sigma$, and $\omega_a = 0.9\omega_\sigma$.

V. INFLUENCE OF THE SPECIAL MODE FORMATION ON THE LASING THRESHOLD AND THE GENERATION FREQUENCY

To quantify the influence of the homogeneous and inhomogeneous broadening on the laser operation, we find the lasing threshold and the generation frequency in a laser where both homogeneous and inhomogeneous broadening exist (see Appendix and Section Method in [59]). We consider the case when $\omega_\sigma^{(j)}$ and Ω_j are independent random variables.

In the resonant case, $\omega_a = \omega_\sigma$, the generation frequency, ω_g , is equal to ω_a and the lasing threshold is given by the following expression:

$$D_0 = D_{\text{th}} = \frac{\gamma_a \Delta\omega}{N\Omega^2} \sqrt{\frac{2}{\pi}} \frac{\exp(-\gamma_\sigma^2/2\Delta\omega^2)}{\text{erfc}(\gamma_\sigma/\sqrt{2}\Delta\omega)}. \quad (5)$$

Here $\text{erfc}(x) = 1 - \frac{2}{\sqrt{\pi}} \int_0^x \exp(-t^2) dt$ is the complementary error function [60] and D_0 is determined by the pump rate as $D_0 = (\gamma_P - \gamma_D)/(\gamma_P + \gamma_D)$. Ω^2 is the average value of squared coupling strengths, Ω_j^2 .

Two notable limiting cases can be obtained from Eq. (5). For $\gamma_\sigma \gg \Delta\omega$ Eq. (5) reduces to the following equation:

$$D_{\text{th}} = \frac{\gamma_\sigma \gamma_a}{N\Omega^2}. \quad (6)$$

Here we use the fact that, in the limit when x tends to infinity, $\text{erfc}(x) \approx \frac{\exp(-x^2)}{x\sqrt{\pi}}$ [60]. Equation (6) coincides with the well-known expression for the lasing threshold in the case where only homogeneous broadening is present [42].

For $\gamma_\sigma \ll \Delta\omega$ the complementary error function is close to unity [60] and Eq. (5) reduces to

$$D_{\text{th}} = \frac{\gamma_a \Delta\omega}{N\Omega^2} \sqrt{\frac{2}{\pi}}. \quad (7)$$

In the nonresonant case, $\omega_a \neq \omega_\sigma$, the generation frequency, ω_g , depends nonmonotonically on the ratio of the width of the homogeneous broadening to the width of the inhomogeneous broadening (Fig. 4) (see the Appendix for details of calculations). If we assume $\Delta\omega \gg \gamma_\sigma$ and $\Delta\omega \gg |\omega_a - \omega_\sigma|$, the generation frequency is found to be

(see the Appendix)

$$\omega_g = \frac{\sqrt{\frac{\pi}{2}} \Delta\omega \omega_a + \gamma_a \omega_\sigma}{\sqrt{\frac{\pi}{2}} \Delta\omega + \gamma_a}. \quad (8)$$

At the same time, in the leading order in $\frac{\gamma_\sigma}{\Delta\omega}$, the lasing threshold is still determined by Eq. (7) even in the nonresonant case. This is because we assume $\Delta\omega \gg |\omega_a - \omega_\sigma|$, which means that the active medium linewidth is much greater than the detuning, and so the detuning becomes irrelevant for the threshold condition.

In the opposite case, when $\Delta\omega \ll \gamma_\sigma$, the generation frequency in a laser is given by the following expression:

$$\omega_g = \frac{\gamma_\sigma \omega_a + \gamma_a \omega_\sigma}{\gamma_\sigma + \gamma_a}. \quad (9)$$

This expression coincides with the well-known formula for the generation frequency in a laser with homogeneous broadening [42].

Comparing Eq. (6) and Eq. (7), we find that the expressions for the lasing thresholds are the same up to the replacement of γ_σ by $\sqrt{\frac{2}{\pi}} \Delta\omega$. Therefore, an active medium with dominant inhomogeneous broadening has a slightly lower lasing threshold than an active medium with the same spectral width, but originating from homogeneous broadening. At the same time, from Eq. (8) and Eq. (9) it is clear that within the given assumptions the generation frequency is the same up to the replacement of γ_σ by $\sqrt{\frac{2}{\pi}} \Delta\omega$. Therefore, in an active medium with dominant inhomogeneous broadening the generation frequency is closer to the cavity frequency than in an active medium with the same spectral width, but originating from homogeneous broadening. Thus homogeneous and inhomogeneous broadening have slightly different effects on the lasing threshold and the generation frequency. However, the same expressions can be used with reasonable accuracy for systems with dominant homogeneous broadening and dominant inhomogeneous broadening.

VI. CONCLUSION

We have studied the effect of inhomogeneous broadening on the behavior of single mode lasers. We show that there is a critical value of pump rate, at which a special mode forms. This special mode consists of collective oscillations of the electromagnetic field in the cavity mode and of the active atoms with different transition frequencies. Despite inhomogeneous broadening, in this mode the oscillations of all active atoms occur at a single shared frequency. Further increase in the pump rate leads to a decrease in the relaxation rate of the special eigenmode, eventually resulting in lasing. Above the lasing threshold, the special mode dominates the laser spectrum. We demonstrate that due to the frequency matching of contributions of active atom's polarizations in this eigenmode, the inhomogeneous broadening is effectively replaced by a homogeneous broadening and a single mode laser can be described in terms of a homogeneously broadened medium. We suggest a system where this behavior can be observed experimentally independent of lasing.

In terms of behavior, two key features have been identified. First, the inhomogeneously broadened emission slowly

transitions into a single homogeneously broadened mode with a Lorentz spectrum as the laser approaches lasing threshold. Therefore, above the threshold inhomogeneous and homogeneous broadening in the active medium are indistinguishable in the spectrum of a single mode laser. Second, inhomogeneous broadening affects the lasing threshold and the generation frequency in a similar way compared to homogeneous broadening, replacing the active atom homogeneous linewidth in both formulas when the inhomogeneous broadening is dominant. However, the lasing threshold for the inhomogeneously broadened active medium is slightly lower than the one for the homogeneously broadened medium. We attribute this advantage to the fact that the Gaussian shape decays faster away from the peak compared to the Lorentz shape; therefore, for the two distributions with the same full width at half maximum Gaussian distribution is effectively narrower. This finding is valuable for design of low-threshold lasers, where inhomogeneous broadening may result in a lower threshold pump rate than expected.

ACKNOWLEDGMENTS

The study was financially supported by a grant from the Russian Science Foundation (Project No. 22-72-00026). I.V.D. thanks the Foundation for the Advancement of Theoretical Physics and Mathematics "Basis."

APPENDIX: DERIVATION OF THE EXPRESSIONS FOR THE LASING THRESHOLD AND THE GENERATION FREQUENCY

To derive an expression for the lasing threshold we find a condition that enables a nontrivial stationary solution in Eqs. (1) and (2) for constant population inversion, $D_j = D_{th}$, $j = 1, \dots$. We assume that $\omega_a = \omega_\sigma$ and look for a solution in the form $a = a_0 e^{-i\omega_g t}$, $\sigma_j = \sigma_{0j} e^{-i\omega_g t}$, $j = 1, \dots$ (ω_g is a yet unknown generation frequency). Substituting a_0 from Eq. (1) into Eq. (2) we arrive at the condition

$$\sigma_{0j} = \frac{D_{th} \Omega_j \sum_k \Omega_k \sigma_{0k}}{[\gamma_a + i(\omega_a - \omega_g)](\gamma_\sigma + i(\omega_\sigma^{(j)} - \omega_g))}, \quad j = 1, \dots \quad (A1)$$

We proceed to multiply Eq. (A1) by Ω_j for each j and then sum over j (over all active atoms). Existence of a nontrivial solution then demands that

$$\gamma_a + i(\omega_a - \omega_g) = D_{th} \sum_j \frac{\Omega_j^2}{(\gamma_\sigma + i(\omega_\sigma^{(j)} - \omega_g))}. \quad (A2)$$

The imaginary part of Eq. (A2) results in $\omega_g = \omega_a$ for any symmetrical distribution of $\omega_\sigma^{(j)}$ centered around ω_a (as expected in the resonant case). The real part of Eq. (A2) yields

$$\gamma_a = \gamma_\sigma D_{th} \sum_j \frac{\Omega_j^2}{\gamma_\sigma^2 + (\omega_\sigma^{(j)} - \omega_a)^2}. \quad (A3)$$

For a sufficiently large number of active atoms with Gaussian distribution (a typical case for an inhomogeneously broadened medium [18,24,25]) and $\omega_a \gg \Delta\omega, \gamma_\sigma, \gamma_a$ we can transform the sum in Eq. (A3) into an integral over

frequencies. We assume that random values Ω_j and $\omega_\sigma^{(j)}$ are independently distributed (see our assumptions in Sec. V), which, for large numbers of atoms, results in expression

$$\gamma_a = \Omega^2 \gamma_\sigma D_{\text{th}} \int_{-\infty}^{+\infty} \frac{N dx}{\Delta\omega} \frac{1}{\gamma_\sigma^2 + x^2} \frac{\exp(-x^2/2\Delta\omega^2)}{\sqrt{2\pi}}. \quad (\text{A4})$$

Here, Ω^2 is the average value of squared coupling strengths, Ω_j^2 .

The integral in Eq. (A4) can be obtained analytically [60], which results in

$$D_{\text{th}} = \frac{\gamma_a \Delta\omega}{N \Omega^2} \sqrt{\frac{2}{\pi}} \frac{\exp(-\gamma_\sigma^2/2\Delta\omega^2)}{\text{erfc}(\gamma_\sigma/\sqrt{2}\Delta\omega)}, \quad (\text{A5})$$

where $\text{erfc}(x) = 1 - \frac{2}{\sqrt{\pi}} \int_0^x \exp(-t^2) dt$ is the complementary error function [60].

Now we derive expressions for the nonresonant case. First, we need to identify the generation frequency. We divide the real part of Eq. (A2) by the imaginary part of Eq. (A2) to exclude D_{th} and obtain the relation for the generation frequency ω_g :

$$\frac{\gamma_a}{\omega_a - \omega_g} = - \frac{\sum_j \frac{\gamma_\sigma}{\gamma_\sigma^2 + (\omega_\sigma^{(j)} - \omega_g)^2}}{\sum_j \frac{\omega_\sigma^{(j)} - \omega_g}{\gamma_\sigma^2 + (\omega_\sigma^{(j)} - \omega_g)^2}}. \quad (\text{A6})$$

These sums are then transformed into integrals in the same way as the transition from Eq. (A5) to Eq. (A6):

$$\frac{\gamma_a}{\omega_a - \omega_g} = \frac{\int_{-\infty}^{\infty} \frac{\gamma_\sigma \exp[-(x-\omega_\sigma)^2/2\Delta\omega^2] dx}{\gamma_\sigma^2 + (x-\omega_\sigma)^2}}{\int_{-\infty}^{\infty} \frac{(x-\omega_\sigma) \exp[-(x-\omega_\sigma)^2/2\Delta\omega^2] dx}{\gamma_\sigma^2 + (x-\omega_\sigma)^2}}. \quad (\text{A7})$$

Note that ω_σ is the center of $\omega_\sigma^{(j)}$ distribution. We will focus on finding the right side of Eq. (A7). Integrals can be calculated as [60]

$$\begin{aligned} & \frac{\gamma_a}{\omega_a - \omega_g} \\ &= i \frac{\text{erfc} \frac{\gamma_\sigma - i(\omega_g - \omega_\sigma)}{\sqrt{2}\Delta\omega} + \exp \frac{2i\gamma_\sigma(\omega_g - \omega_\sigma)}{\Delta\omega^2} \text{erfc} \frac{\gamma_\sigma + i(\omega_g - \omega_\sigma)}{\sqrt{2}\Delta\omega}}{\text{erfc} \frac{\gamma_\sigma - i(\omega_g - \omega_\sigma)}{\sqrt{2}\Delta\omega} - \exp \frac{2i\gamma_\sigma(\omega_g - \omega_\sigma)}{\Delta\omega^2} \text{erfc} \frac{\gamma_\sigma + i(\omega_g - \omega_\sigma)}{\sqrt{2}\Delta\omega}}. \end{aligned} \quad (\text{A8})$$

In general, Eq. (A8) can be solved numerically to obtain ω_g ; however, a useful limit can be obtained if we assume that the inhomogeneous broadening is larger than the homogeneous broadening, $\Delta\omega \gg \gamma_\sigma$, and the frequency detuning, $\Delta\omega \gg |\omega_g - \omega_\sigma|$ (the latter is satisfied if, e.g., $\Delta\omega \gg |\omega_a - \omega_\sigma|$, since the generation frequency ω_g lies between ω_a and ω_σ). In this case, the complementary error functions and exponents in Eq. (A8) are estimated as two leading orders of their Taylor series, which results in

$$\frac{\gamma_a}{\omega_a - \omega_g} = \sqrt{\frac{\pi}{2}} \frac{\Delta\omega}{\omega_g - \omega_\sigma}. \quad (\text{A9})$$

After trivial algebra we obtain

$$\omega_g = \frac{\sqrt{\pi/2} \Delta\omega \omega_a + \gamma_a \omega_\sigma}{\sqrt{\pi/2} \Delta\omega + \gamma_a}. \quad (\text{A10})$$

Inserting Eq. (A10) into the real part of Eq. (A2) results in the same threshold condition [see Eq. (7)]. The reason why detuning between electromagnetic field and active medium does not affect the threshold in our derivation is because we assume $\Delta\omega \gg |\omega_g - \omega_\sigma|$ to obtain Eq. (A10), i.e., the active medium linewidth is much greater than the detuning, and thus the latter does not play a notable role.

-
- [1] C. Wehrenfennig, M. Liu, H. J. Snaith, M. B. Johnston, and L. M. Herz, Homogeneous emission line broadening in the organo lead halide perovskite $\text{CH}_3\text{NH}_3\text{PbI}_{3-x}\text{Cl}_x$, *J. Phys. Chem. Lett.* **5**, 1300 (2014).
- [2] J. G. Bartholomew, K. de Oliveira Lima, A. Ferrier, and P. Goldner, Optical line width broadening mechanisms at the 10 kHz level in $\text{Eu}^{3+}:\text{Y}_2\text{O}_3$ nanoparticles, *Nano Lett.* **17**, 778 (2017).
- [3] R. Sarkar, P. Ahuja, P. R. Vasos, and G. Bodenhausen, Long-lived coherences for homogeneous line narrowing in spectroscopy, *Phys. Rev. Lett.* **104**, 053001 (2010).
- [4] G. Moody, C. K. Dass, K. Hao, C.-H. Chen, L.-J. Li, A. Singh, K. Tran, G. Clark, X. Xu, and G. Berghäuser, Intrinsic homogeneous linewidth and broadening mechanisms of excitons in monolayer transition metal dichalcogenides, *Nat. Commun.* **6**, 8315 (2015).
- [5] F. Cadiz, E. Courtade, C. Robert, G. Wang, Y. Shen, H. Cai, T. Taniguchi, K. Watanabe, H. Carrere, D. Lagarde, M. Manca, T. Amand, P. Renucci, S. Tongay, X. Marie, and B. Urbaszek, Excitonic linewidth approaching the homogeneous limit in MoS_2 -based van der Waals heterostructures, *Phys. Rev. X* **7**, 021026 (2017).
- [6] E. U. Rafailov, M. A. Cataluna, and W. Sibbett, Mode-locked quantum-dot lasers, *Nat. Photon.* **1**, 395 (2007).
- [7] M. R. Salvador, M. A. Hines, and G. D. Scholes, Exciton-bath coupling and inhomogeneous broadening in the optical spectroscopy of semiconductor quantum dots, *J. Chem. Phys.* **118**, 9380 (2003).
- [8] S. S. Savchenko and I. A. Weinstein, Inhomogeneous broadening of the exciton band in optical absorption spectra of InP/ZnS nanocrystals, *Nanomaterials* **9**, 716 (2019).
- [9] J. C. van der Bok, D. M. Dekker, M. L. J. Peerlings, B. V. Salzmann, and A. Meijerink, Luminescence line broadening of CdSe nanoplatelets and quantum dots for application in w-LEDs, *J. Phys. Chem. C* **124**, 12153 (2020).
- [10] S. Kabi and A. G. U. Perera, Effect of quantum dot size and size distribution on the intersublevel transitions and absorption coefficients of III-V semiconductor quantum dot, *J. Appl. Phys.* **117**, 124303 (2015).
- [11] I. Y. Chestnov, V. A. Shahnazaryan, A. P. Alodjants, and I. A. Shelykh, Terahertz lasing in ensemble of asymmetric quantum dots, *ACS Photon.* **4**, 2726 (2017).
- [12] T. R. Tan, R. Kaewuam, K. J. Arnold, S. R. Chanu, Z. Zhang, M. S. Safronova, and M. D. Barrett, Suppressing

- inhomogeneous broadening in a lutetium multi-ion optical clock, *Phys. Rev. Lett.* **123**, 063201 (2019).
- [13] H. Q. Fan, K. H. Kagalwala, S. V. Polyakov, A. L. Migdall, and E. A. Goldschmidt, Electromagnetically induced transparency in inhomogeneously broadened solid media, *Phys. Rev. A* **99**, 053821 (2019).
- [14] P. Andrejić and A. Pálffy, Superradiance and anomalous hyperfine splitting in inhomogeneous ensembles, *Phys. Rev. A* **104**, 033702 (2021).
- [15] N. M. Abishev, E. I. Baibekov, B. Z. Malkin, M. N. Popova, D. S. Pytalev, and S. A. Klimin, Deformation broadening and the fine structure of spectral lines in optical spectra of dielectric crystals containing rare-earth ions, *Phys. Solid State* **61**, 795 (2019).
- [16] E. F. Petrushevich, M. H. E. Bousquet, B. Ośmiałowski, D. Jacquemin, J. M. Luis, and R. Zalesny, Cost-effective simulations of vibrationally-resolved absorption spectra of fluorophores with machine-learning-based inhomogeneous broadening, *J. Chem. Theory Comput.* **19**, 2304 (2023).
- [17] J. Cerezo, F. J. A. Ferrer, G. Prampolini, and F. Santoro, Modeling solvent broadening on the vibronic spectra of a series of coumarin dyes. From implicit to explicit solvent models, *J. Chem. Theory Comput.* **11**, 5810 (2015).
- [18] F. J. A. Ferrer, R. Improta, F. Santoro, and V. Barone, Computing the inhomogeneous broadening of electronic transitions in solution: A first-principle quantum mechanical approach, *Phys. Chem. Chem. Phys.* **13**, 17007 (2011).
- [19] H. E. Tureci, A. D. Stone, and B. Collier, Self-consistent multi-mode lasing theory for complex or random lasing media, *Phys. Rev. A* **74**, 043822 (2006).
- [20] M. L. Andersen, S. Stobbe, A. S. Sørensen, and P. Lodahl, Strongly modified plasmon-matter interaction with mesoscopic quantum emitters, *Nat. Phys.* **7**, 215 (2011).
- [21] M. I. Khan, M. Idrees, B. A. Bacha, H. Khan, A. Ullah, and M. Haneef, Optical soliton through induced cesium doppler broadening medium, *Phys. Scr.* **95**, 085102 (2020).
- [22] A. M. Ismail, M. I. Mohammed, and S. S. Fouad, Optical and structural properties of polyvinylidene fluoride (PVDF)/reduced graphene oxide (RGO) nanocomposites, *J. Mol. Struct.* **1170**, 51 (2018).
- [23] V. C. Chen, *The Micro-Doppler Effect in Radar* (Artech House, Boston, 2019).
- [24] S. T. Hoffmann, H. Bassler, and A. Kohler, What determines inhomogeneous broadening of electronic transitions in conjugated polymers? *J. Phys. Chem. B* **114**, 17037 (2010).
- [25] M. E. Reimer, G. Bulgarini, A. Fognini, R. W. Heeres, B. J. Witek, M. A. M. Versteegh, A. Rubino, T. Braun, M. Kamp, S. Höfling, D. Dalacu, J. Lapointe, P. J. Poole, and V. Zwiller, Overcoming power broadening of the quantum dot emission in a pure wurtzite nanowire, *Phys. Rev. B* **93**, 195316 (2016).
- [26] V. V. Petrov, *Sums of Independent Random Variables* (Springer Science & Business Media, New York, 2012), Vol. 82.
- [27] M. A. Zentile, J. Keaveney, R. S. Mathew, D. J. Whiting, C. S. Adams, and I. G. Hughes, Optimization of atomic faraday filters in the presence of homogeneous line broadening, *J. Phys. B* **48**, 185001 (2015).
- [28] C. Sun, V. Y. Chernyak, A. Piryatinski, and N. A. Sinitsyn, Cooperative light emission in the presence of strong inhomogeneous broadening, *Phys. Rev. Lett.* **123**, 123605 (2019).
- [29] K. Debnath, Y. Zhang, and K. Mølmer, Collective dynamics of inhomogeneously broadened emitters coupled to an optical cavity with narrow linewidth, *Phys. Rev. A* **100**, 053821 (2019).
- [30] R. Houdre, R. P. Stanley, and M. Hegems, Vacuum-field Rabi splitting in the presence of inhomogeneous broadening: Resolution of a homogeneous linewidth in an inhomogeneously broadened system, *Phys. Rev. A* **53**, 2711 (1996).
- [31] I. Diniz, S. Portolan, R. Ferreira, J. M. Gérard, P. Bertet, and A. Auffèves, Strongly coupling a cavity to inhomogeneous ensembles of emitters: Potential for long-lived solid-state quantum memories, *Phys. Rev. A* **84**, 063810 (2011).
- [32] N. Mermilliod, R. Romero, I. Chartier, C. Garapon, and R. Moncorgé, Performance of various diode-pumped Nd: Laser materials: influence of inhomogeneous broadening, *IEEE J. Quantum Electron.* **28**, 1179 (1992).
- [33] L. C. Andreani, G. Panzarini, A. V. Kavokin, and M. R. Vladimirova, Effect of inhomogeneous broadening on optical properties of excitons in quantum wells, *Phys. Rev. B* **57**, 4670 (1998).
- [34] A. A. Zyablovsky, I. V. Doronin, E. S. Andrianov, A. A. Pukhov, Y. E. Lozovik, A. P. Vinogradov, and A. A. Lisyansky, Exceptional points as lasing prethresholds, *Laser Photon. Rev.* **15**, 2000450 (2021).
- [35] C. V. Shank, Physics of dye lasers, *Rev. Mod. Phys.* **47**, 649 (1975).
- [36] A. Zenner, E. Beham, S. Stuffer, F. Findeis, M. Bichler, and G. Abstreiter, Coherent properties of a two-level system based on a quantum-dot photodiode, *Nature (London)* **418**, 612 (2002).
- [37] Y.-M. He, H. Wang, C. Wang, M.-C. Chen, X. Ding, J. Qin, Z.-C. Duan, S. Chen, J.-P. Li, R.-Z. Liu, C. Schneider, M. Atatüre, S. Höfling, C.-Y. Lu, and J.-W. Pan, Coherently driving a single quantum two-level system with dichromatic laser pulses, *Nat. Phys.* **15**, 941 (2019).
- [38] W. Cartar, J. Mørk, and S. Hughes, Self-consistent Maxwell-Bloch model of quantum-dot photonic-crystal-cavity lasers, *Phys. Rev. A* **96**, 023859 (2017).
- [39] D. Meiser, J. Ye, D. R. Carlson, and M. J. Holland, Prospects for a Millihertz-Linewidth laser, *Phys. Rev. Lett.* **102**, 163601 (2009).
- [40] J. G. Bohnet, Z. Chen, J. M. Weiner, D. Meiser, M. J. Holland, and J. K. Thompson, A steady-state superradiant laser with less than one intracavity photon, *Nature (London)* **484**, 78 (2012).
- [41] H. Haken, *Laser Light Dynamics* (North-Holland, Amsterdam, 1985), Vol. 2.
- [42] M. O. Scully and M. S. Zubairy, *Quantum Optics* (Cambridge University Press, Cambridge, UK, 1997).
- [43] A. E. Siegman, *Lasers* (University Science Books, Mill Valley, CA, 1986), p. 654.
- [44] A. Narayanaswamy, L. F. Feiner, A. Meijerink, and P. J. V. der Zaag, The effect of temperature and dot size on the spectral properties of colloidal inP/ZnS core-shell quantum dots, *ACS Nano* **3**, 2539 (2009).
- [45] P. Borri, W. Langbein, S. Schneider, U. Woggon, R. L. Sellin, D. Ouyang, and D. Bimberg, Ultralong dephasing time in InGaAs quantum dots, *Phys. Rev. Lett.* **87**, 157401 (2001).
- [46] D. Birkedal, K. Leosson, and J. M. Hvam, Long lived coherence in self-assembled quantum dots, *Phys. Rev. Lett.* **87**, 227401 (2001).

- [47] M. Bayer and A. Forchel, Temperature dependence of the exciton homogeneous linewidth in $\text{In}_{0.60}\text{Ga}_{0.40}\text{As}/\text{GaAs}$ self-assembled quantum dots, *Phys. Rev. B* **65**, 041308(R) (2002).
- [48] S. Das and M. A. Macovei, Collective quantum dot inversion and amplification of photon and phonon waves, *Phys. Rev. B* **88**, 125306 (2013).
- [49] J. H. Quilter, A. J. Brash, F. Liu, M. Glässl, A. M. Barth, V. M. Axt, A. J. Ramsay, M. S. Skolnick, and A. M. Fox, Phonon-assisted population inversion of a single $\text{InGaAs}/\text{GaAs}$ quantum dot by pulsed laser excitation, *Phys. Rev. Lett.* **114**, 137401 (2015).
- [50] Y. I. Khanin, *Principles of Laser Dynamics* (Newnes, London, 2012).
- [51] T. Pickering, J. M. Hamm, A. F. Page, S. Wuestner, and O. Hess, Cavity-free plasmonic nanolasing enabled by dispersionless stopped light, *Nat. Commun.* **5**, 4972 (2014).
- [52] A. P. Vinogradov, E. S. Andrianov, A. A. Pukhov, A. V. Dorofeenko, and A. A. Lisyansky, Quantum plasmonics of metamaterials: loss compensation using spasers, *Phys.-Usp.* **55**, 1046 (2012).
- [53] I. V. Doronin, A. A. Zyablovsky, E. S. Andrianov, A. A. Pukhov, and A. P. Vinogradov, Lasing without inversion due to parametric instability of the laser near the exceptional point, *Phys. Rev. A* **100**, 021801(R) (2019).
- [54] I. V. Doronin, A. A. Zyablovsky, and E. S. Andrianov, Strong-coupling-assisted formation of coherent radiation below the lasing threshold, *Opt. Express* **29**, 5624 (2021).
- [55] A. A. Zyablovsky, E. S. Andrianov, I. A. Nechepurenko, A. V. Dorofeenko, A. A. Pukhov, and A. P. Vinogradov, Approach for describing spatial dynamics of quantum light-matter interaction in dispersive dissipative media, *Phys. Rev. A* **95**, 053835 (2017).
- [56] A. A. Zyablovsky, I. A. Nechepurenko, E. S. Andrianov, A. V. Dorofeenko, A. A. Pukhov, A. P. Vinogradov, and A. A. Lisyansky, Optimum gain for plasmonic distributed feedback lasers, *Phys. Rev. B* **95**, 205417 (2017).
- [57] F. van Beijnum, P. J. van Veldhoven, E. J. Geluk, M. J. A. de Dood, G. W. 't Hooft, and M. P. van Exter, Surface plasmon lasing observed in metal hole arrays, *Phys. Rev. Lett.* **110**, 206802 (2013).
- [58] N. E. Nefedkin, A. A. Zyablovsky, E. S. Andrianov, A. A. Pukhov, and A. P. Vinogradov, Mode cooperation in a two-dimensional plasmonic distributed-feedback laser, *ACS Photon.* **5**, 3031 (2018).
- [59] I. V. Doronin, A. A. Zyablovsky, E. S. Andrianov, A. A. Pukhov, Y. E. Lozovik, and A. P. Vinogradov, Universal lasing condition, *Sci. Rep.* **11**, 4197 (2021).
- [60] M. Abramowitz and I. A. Stegun, *Handbook of Mathematical Functions with Formulas, Graphs, and Mathematical Tables* (US GPO, New York, 1968), Vol. 55.